

Isolation and Characterization of Cellulose Nanocrystals from *Agave angustifolia* Fibre

Noor Afizah Rosli, Ishak Ahmad,* and Ibrahim Abdullah

Cellulose nanocrystals were extracted from *Agave angustifolia* fibres by alkali and bleaching treatments followed by acid hydrolysis. The chemical composition of the *Agave* fibres was determined at different stages of chemical treatment. The structural analysis was carried out by a Fourier Transform Infrared spectroscopy and X-ray diffraction. The morphology and thermal stability of the *Agave* fibres at different stages of chemical treatment were investigated by field emission scanning electron microscopy and thermogravimetric analysis, respectively. The results indicated that the hemicellulose and lignin were removed extensively from the extracted cellulose. The two peaks at 1735 cm^{-1} and 1247 cm^{-1} , which were attributed to the C=O stretching and C-O out of plane stretching vibration of the hemicellulose and lignin in raw *Agave*, completely disappeared in the spectra of chemically treated fibres. The X-ray diffraction data showed enrichment in the portion of crystalline cellulose from 59% to 82% in the raw and cellulose nanocrystals, respectively. Thermogravimetric analysis showed that the thermal stability improved significantly by various chemical stages. The size reduction of the *Agave* cellulose into nano-sized particles from $7\text{ }\mu\text{m}$ to 8 nm in diameter by acid hydrolysis was confirmed with transmission electron microscopy images.

Keywords: Acid hydrolysis; Cellulose; Nanocrystals; Natural fibres

Contact information: Polymer Research Centre (PORCE), School of Chemical Sciences and Food Technology, Faculty of Science and Technology, Universiti Kebangsaan Malaysia, 43600 Bangi Selangor, Malaysia; *Corresponding author: gading@ukm.my

INTRODUCTION

Biocomposites processing using natural fibres as reinforcement has increased dramatically in recent years (Jiang and Hinrichsen 1999; Luo and Netravali 1999; Takagi and Asano 2008; Takagi and Ichihara 2004). In addition, natural fibres have found extensive applications in textiles, paper manufacturing, building, and civil engineering fields (Kalia *et al.* 2009).

Natural fibres of lignocellulosic materials can be classified according to their plant origin *i.e.*: (i) bast or stem, (ii) leaf, (iii) seed or fruit, (iv) grass, and (v) straw fibres. Natural fibres have many advantages over man-made fibres, such as low density, low cost, availability, renewability, biodegradability, and low abrasivity (Bledzki *et al.* 1996). A better understanding of the chemical, mechanical, and physical properties of natural fibres is necessary for processing natural fibre-reinforced composites. Natural fibres consist of cellulose, hemicelluloses, lignin, pectin, waxes, and water soluble substances. Cellulose is a semi-crystalline polysaccharide consisting of D-glucopyranosyl units linked together by β -(1-4)-glucosidic bonds (Bledzki and Gassan 1999). Three hydroxyl groups, at the C2 and C3 positions of secondary hydroxyl groups, and the C6 position of

primary hydroxyl groups, can form intra- and intermolecular hydrogen bonds. These hydrogen bonds allow the creation of highly ordered, three dimensional crystal structures (Abdul Khalil *et al.* 2011). Lignin is a polymer of phenylpropane units which are highly complex, mainly aromatic and amorphous, but have less water sorption than other natural fibre components (Rowell *et al.* 1997). Hemicellulose is branched, fully amorphous, and has a lower molecular weight than cellulose; as a consequence it is partly soluble in water. Hemicellulose is hygroscopic due to its open structure containing hydroxyl and acetyl groups (Frederick and Norman 2004).

The purpose of this study was to produce cellulose nanocrystals (CNCs) from *Agave angustifolia* as a substitute for synthetic fibres to make a good economic and ecologic composite material. The term “cellulose nanocrystal” is used to designate elongated crystalline rod-like cellulose nanoparticles. *Agave angustifolia* belongs to the Agavaceae family and is one of 140 species of the *Agave* genus. *Agave angustifolia* is known as the “Century Plant” or locally named as “Kelumpang Telur”. The leaf of *A. angustifolia* is about 1½ inches wide with creamy yellow stripes along the spiny margins as shown in Fig. 1. The plant grows into a spherical clump of 3 to 4 feet in diameter. This species can tolerate full sun, part shade, and reflected heat. It can also handle more water than most *Agave* species. It has been utilized by people for domestic purposes such as making rope, soap, and other products. Although the leaves are widely used, no studies on the extraction or properties of the cellulose fibres from these leaves have been conducted to date.



Fig. 1. Photograph of *Agave angustifolia* plants

CNCs have great potential as reinforcing agents in nanocomposites due to their size and the possibility of chemically modifying their surface. It is known that the conventional CNC exhibits high stiffness and modulus, which can be as high as 134 GPa (Okスマン and Sain 2006). It has been stated that the crystal structure exhibits a tensile strength from 0.8 up to 10 GPa (Nishino *et al.* 1995).

A well known process for the isolation of CNCs is strong acid hydrolysis. It allows the removal of the form crystalline nanoparticles. Many researchers have recently used this method to prepare CNCs, from kenaf (Kargarzadeh *et al.* 2012), banana plant

(Elanthikkal *et al.* 2010), coconut husk (Rosa *et al.* 2010), rice husk (Johar *et al.* 2012), and sugarcane bagasse (Mandal and Chakrabarty 2011).

In this study, cellulose and CNCs were extracted from *Agave* fibres by chemical methods of alkali and bleaching treatments followed by acid hydrolysis. The next study aims for the application of cellulose and CNCs of *Agave* fibre in biocomposites. Thus, investigations on the chemical and physical properties were carried out to analyse their suitability as reinforcing agent in biocomposites.

EXPERIMENTAL

Materials

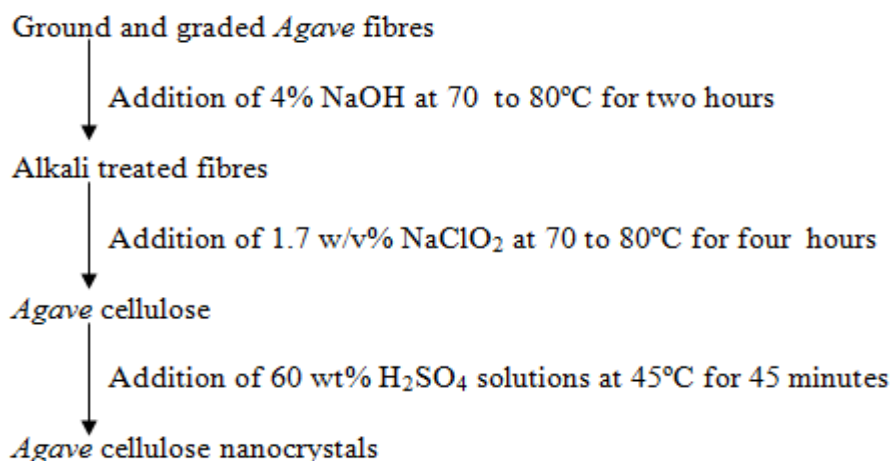
Agave leaves used in this study were harvested in Kajang, Selangor (Malaysia). The chemical reagents used were sodium chlorite (NaClO_2 , Sigma-Aldrich), acetic acid glacial (99%, System), sodium hydroxide (NaOH , System), sulphuric acid (H_2SO_4 , 98%, Univar), methanol (R&M Chemicals), toluene (System), and acetone (System).

Extraction of Cellulose

The thorns on the mature *Agave* leaf margin and tips were removed. The leaves were dried for three days to remove excess moisture. *Agave* fibres were extracted from the leaves using fibre extracting machine and were retted for one week. Then the fibres were combed and shadow-dried for 4 h. The long fibres were cut to 3 to 5 cm and ground using a mill. The ground fibres were treated with 4% NaOH at 70 to 80 °C for 2 h, after which bleaching treatment was carried out using 1.7 w/v% NaClO_2 at 70 to 80 °C for 4 h. The ratio of the fibres to liquor was 1:25 (g/mL). Each fibre treatment was done twice, and the fibres were washed with distilled water after each treatment.

Isolation of Cellulose Nanocrystals

Scheme 1 depicts the methodology routes to obtained CNCs from *Agave* fibres. The hydrolysis was carried out using 60 wt% H_2SO_4 solutions at 45 °C for 45 min. The ratio of the obtained cellulose to liquor was 1:20 (wt%).



Scheme 1. Scheme for CNCs production from *Agave* fibre

The hydrolyzed cellulose was washed five times by centrifugation (10,000 rpm, 10 min, and 10 °C). After washing, the products were neutralized with 2 N NaOH to a pH of 7. The neutralized products were further washed three more times. The suspension was then dialyzed against distilled water to a constant pH.

Determination of Chemical Composition

The chemical composition of the *Agave* fibres before and after the chemical treatment was determined. Dewaxing was carried out by boiling the fibres in a mixture of toluene/methanol (1:1 v/v) in a sachet for 6 h. The de-waxed fibres were then filtered, washed with methanol, and dried. The percentage of holocellulose was calculated according to the method described previously (Wise *et al.* 1946). In this method, the extracted residue of de-waxed fibres was boiled in a mixture of NaClO₂ and acetic acid for 4 h. The suspension was cooled in an ice bath for 30 min, filtered, and washed with cold distilled water. Finally, it was washed with acetone and dried. The α -cellulose and the acid-insoluble lignin content was determined according to TAPPI standard methods T203 and T222, respectively.

Field Emission Scanning Electron Microscopy

Field emission scanning electron (FESEM) micrographs of the treated and untreated fibres were recorded on a Zeiss Supra 55VP microscope at a voltage of 3 kV. The micrographs of the longitudinal and cross section of the *Agave* leaves were also recorded. The samples were coated with gold to avoid charging.

Transmission Electron Microscopy

In order to determine the dimensions of the CNCs, the hydrolyzed suspension were analyzed by a Philips CM12 transmission electron microscope (TEM) operating at 80 kV. A drop of a highly diluted suspension of CNCs was placed on a copper grid coated with a thin carbon film and allowed to dry at room temperature. The copper grid was then stained with a 2 wt% solution of uranyl acetate for one minute and air dried.

Fourier Transform Infrared Spectroscopy

The Fourier transform infrared (FTIR) spectra of the *Agave* fibres were recorded on a Perkin-Elmer spectrometer (SpectrumGX) in the range 500 to 4000 cm⁻¹ with a scanning resolution of 8 cm⁻¹. Before analysis, all of the samples were ground into a fine powder and dried for 24 h at 60 °C in an oven. The ground fibres was mixed with KBr, and pressed into an ultra-thin pellet.

X-ray Diffraction

X-ray diffraction (XRD) analysis was performed with a Bruker AXS D8 Advance diffractometer at 40 kV, 40 mA with Cu-K α radiation ($\lambda=0.1541$ nm). Before analysis, the samples were ground into a fine powder using a mill and pressed into a sample holder. The data was acquired in a 2θ range from 5 to 60°. The crystallinity index (I_c) of *Agave* fibres at different chemical stages was calculated using the following formula (Segal *et al.* 1959).

$$I_c = \frac{I_{002} - I_{am}}{I_{002}} \times 100 \quad (1)$$

where I_{002} is maximum intensity of diffraction of the (002) lattice peak (22° to 23°), and I_{am} is that of the amorphous material between 18° to 19° where the intensity is minimum.

Thermogravimetric Analysis

A Mettler Toledo model TGA/SDTA851e thermogravimetric analyzer was used to characterize the thermal stability of the *Agave* fibres. Approximately 2 mg of each sample was placed in an aluminium pan and heated from 30 to 600 °C at a heating rate of 10 °C/min. All of the measurements were performed under a nitrogen atmosphere.

RESULT AND DISCUSSION

Chemical Composition

The chemical compositions of raw, alkali treated, and bleached *Agave* fibres are presented in Table 1. The raw *Agave* fibres are composed of 67.0% cellulose, 25.2% hemicelluloses, 6.3% lignin, and 2.5% extractives. The amount of hemicelluloses and lignin are higher in raw fibre as compared to the treated fibres. NaOH was found to be efficient in removing the hemicellulose from the fibre, as hemicellulose content was decreased from 25.2% to 3.9%. Based on the chemical composition analysis, most of the lignin content was removed by the bleaching treatment, in which it reacts with NaClO_2 to dissolve as a lignin chloride. Bleaching does not only remove lignin, but also some of the hemicellulose. The final fibre obtained after the bleaching treatment was found to have the highest cellulose content (97.3%).

Table 1. Chemical Composition of *Agave* Fibres at Different Stages of Chemical Treatment

Fibre stage	α -cellulose (%)	Hemicellulose (%)	Lignin (%)	Extractives (%)
Raw	67.01 ± 0.15	25.18 ± 0.98	6.25 ± 0.01	2.50 ± 0.26
Alkali treated	87.95 ± 0.29	3.91 ± 0.92	6.00 ± 0.04	-
Bleached	97.31 ± 0.02	3.14 ± 0.35	0.23 ± 0.04	-

Morphological Analysis

Figure 2 shows the *Agave angustifolia* fibres at different stages of the chemical treatment. The colour of the fibres changed from cream to light brown after the alkali treatment, and white after bleaching.

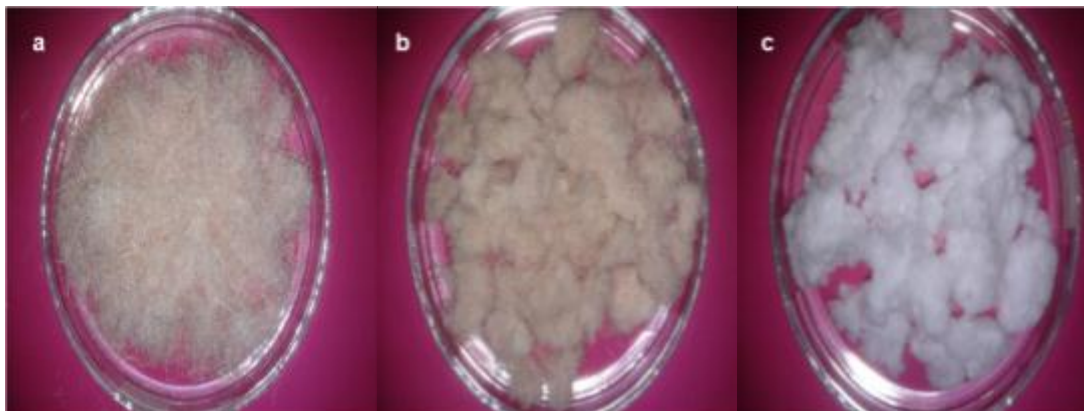


Fig. 2. Photographs of (a) raw, (b) alkali-treated, and (c) bleached *Agave* fibres

Figure 3 shows FESEM micrographs of *Agave* leaves and fibres. Microscopic examinations on the longitudinal and cross section of the leaves are depicted in Figs. 3a and 3b. By examining the longitudinal section of the *Agave* leaves, one can see a 'composite'-like structure in which the fibre bundles are held together by non-cellulosic substances.

Figure 3b shows the cross section of the arch fibres, which are usually found in the middle of the leaf. The arch fibres show an irregular section with a wide variety of sizes of the lumen, and growth in association with the conducting tissue of the plant (Nutman 1936). Xylem fibres are connected to the arch fibres through the conducting tissue and grow opposite to the arch fibres. These fibres run from base to the tip of the plant and give good mechanical strength (Nutman 1936). Nutman (1936) stated that they are composed of thin-walled cells which are broken up during the fibre extraction process. Every fibre contains numerous elongated individual fibres, or fibre cells, and each of them is made up of four main parts (primary wall, the thick secondary wall, tertiary wall, and lumen) as shown in Fig. 3b (Murherjee and Satyanarayana 1984). The fibre cells are linked together by the middle lamellae which consist of hemicelluloses and lignin.

Figures 3c-e presents FESEM micrographs of the raw and chemically treated fibres. From these three micrographs it is clear that the morphology of the fibres changed with the chemical treatment. The changes in the morphology are important to predict the fibres interaction with the polymer matrix in the composites. As shown in Fig. 3c, the raw *Agave* is composed of bundles of continuous individual cells that are bound together by cemented components. The surface of the raw *Agave* was irregular and covered with impurities such as hemicelluloses, lignin, pectin, and waxy substances. The diameter of the raw *Agave* fibres ranged from 60 to 230 μm , and about 59% of them were found to have diameters between 110 to 190 μm .

The results portrayed in Fig. 3d illustrate the surface of the *Agave* fibres after the alkali treatment. It can be seen that the fibre began to look smoother than the raw one as the impurities were removed from the fibre surface. Hemicellulose is hydrolyzed and becomes water-soluble upon the alkali treatment. This phenomenon helps defibrillation and the opening of the fibre bundles as shown in Fig. 3d, with the diameter of the fibrils being reduced to a great extent. The diameter of the *Agave* fibres after the alkali treatment was found to be between 9 to 110 μm .

As seen in Fig. 3e, the bleaching resulted in further defibrillation. The defibrillation already occurred upon the alkali treatment, and this trend increased along with the bleaching treatment due to the removal of the lignin. The bleaching treatment effectively modified the surface of the microfibrils, which appeared smoother than the case of the untreated fibre. After bleaching, the fibre bundles were disintegrated into individual cells with diameters in the range of 7 to 12 μm .

Figures 4(a) and 4(b) show the TEM micrograph and distribution of the diameter, and the aspect ratios of the *Agave* CNCs, respectively. The TEM micrographs demonstrated the efficiency of the acid hydrolysis treatment, which showed the CNCs' needle-like structure consisting mostly of individual fibrils and some aggregates. The CNCs ranged from 8 to 15 nm in diameter and 170 to 500 nm in length, with an average of 10 nm in diameter and 310 nm in length. The calculated aspect ratios of the CNCs were in the range of 10 to 45 with 70% in the range of long CNC; this indicates great potential for them to be used as a reinforcing agent in nanocomposites. The aspect ratios reported here

are similar to those reported on CNCs from other cellulosic sources, such as coconut husk (Rosa *et al.* 2010).

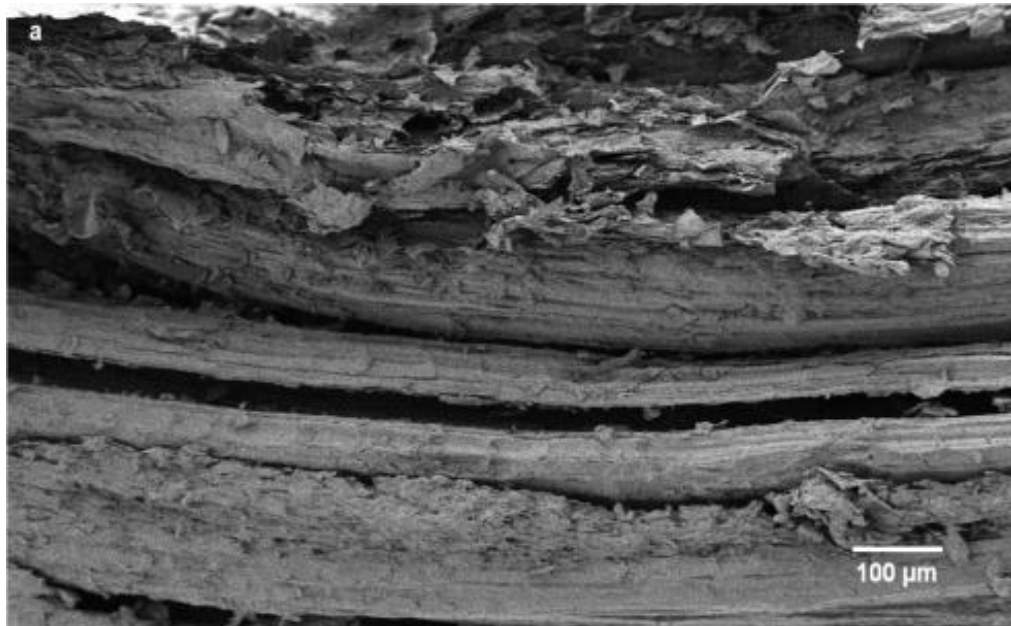


Fig. 3a. FESEM micrographs of *Agave* leaves and fibres: (a) longitudinal section, (b) cross section of the arch (Murherjee and Satyanarayana,1984), (c) raw, (d) alkali-treated, and (e) bleached

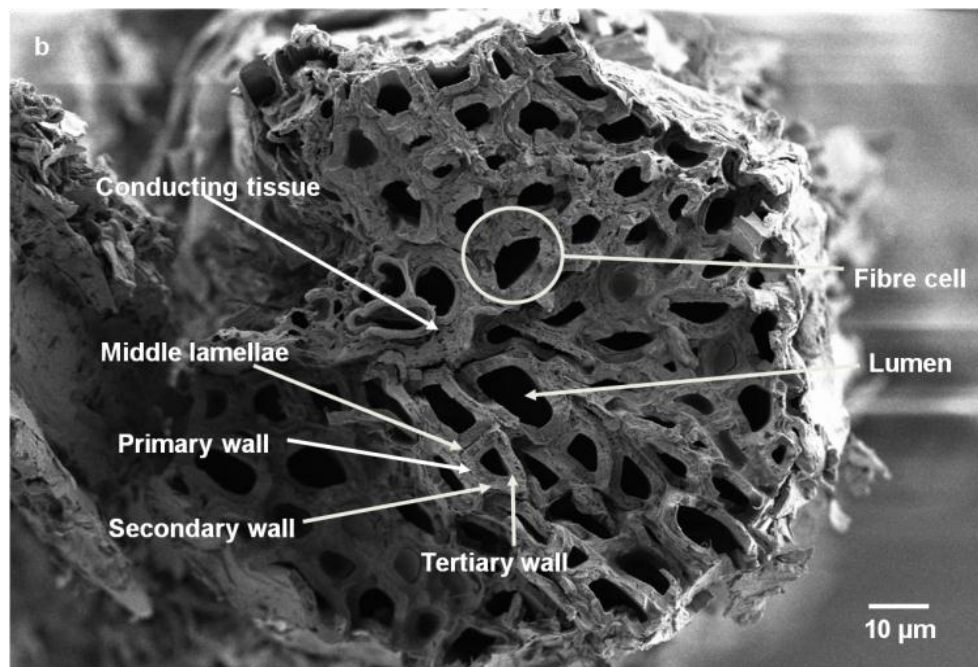


Fig. 3b. FESEM micrographs of *Agave* leaves and fibres: (a) longitudinal section, (b) cross section of the arch (Murherjee and Satyanarayana,1984), (c) raw, (d) alkali-treated, and (e) bleached

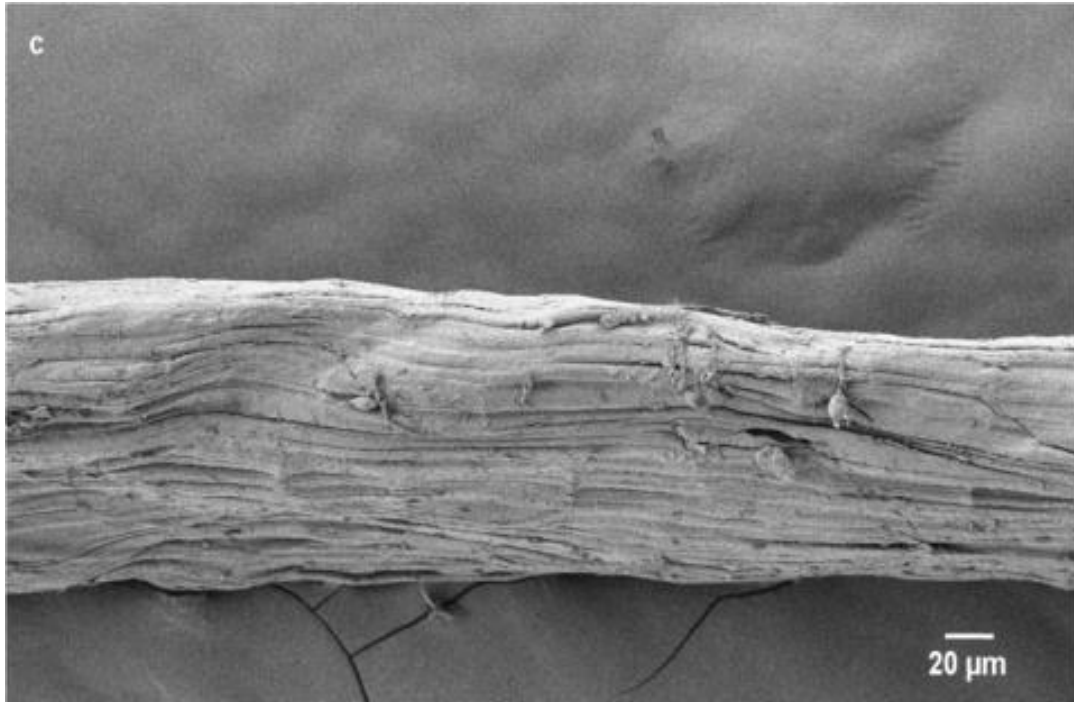


Fig. 3c. FESEM micrographs of *Agave* leaves and fibres: (a) longitudinal section, (b) cross section of the arch (Murherjee and Satyanarayana,1984), (c) raw, (d) alkali-treated, and (e) bleached



Fig. 3d. FESEM micrographs of *Agave* leaves and fibres: (a) longitudinal section, (b) cross section of the arch (Murherjee and Satyanarayana,1984), (c) raw, (d) alkali-treated, and (e) bleached

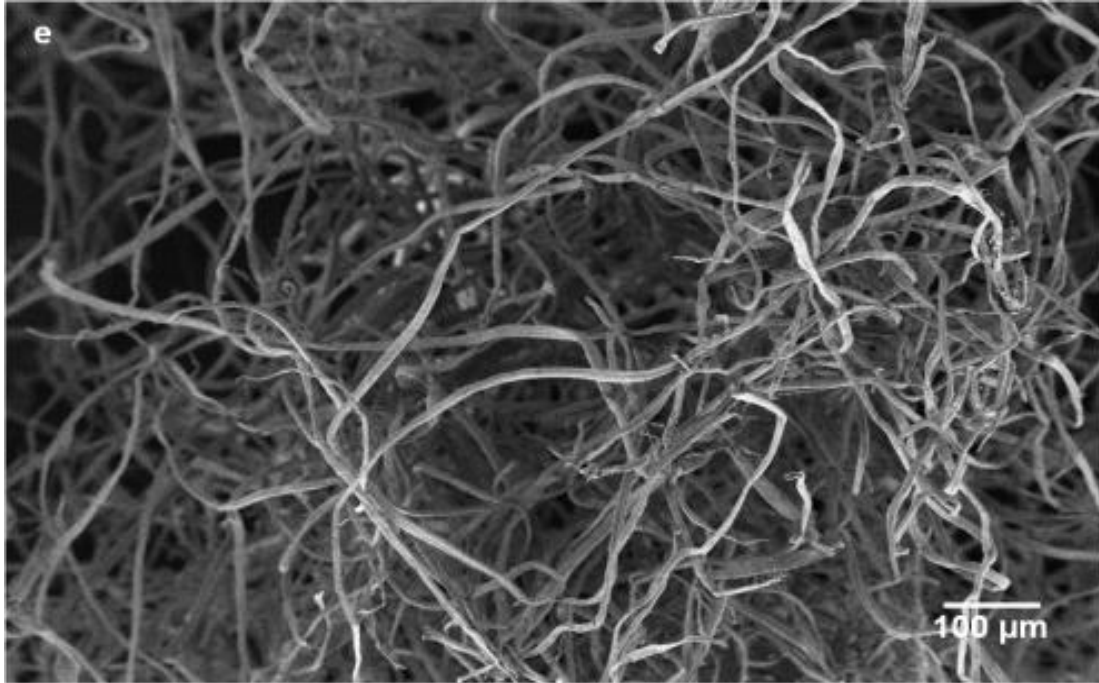


Fig. 3e. FESEM micrographs of *Agave* leaves and fibres: (a) longitudinal section, (b) cross section of the arch (Murherjee and Satyanarayana,1984), (c) raw, (d) alkali-treated, and (e) bleached

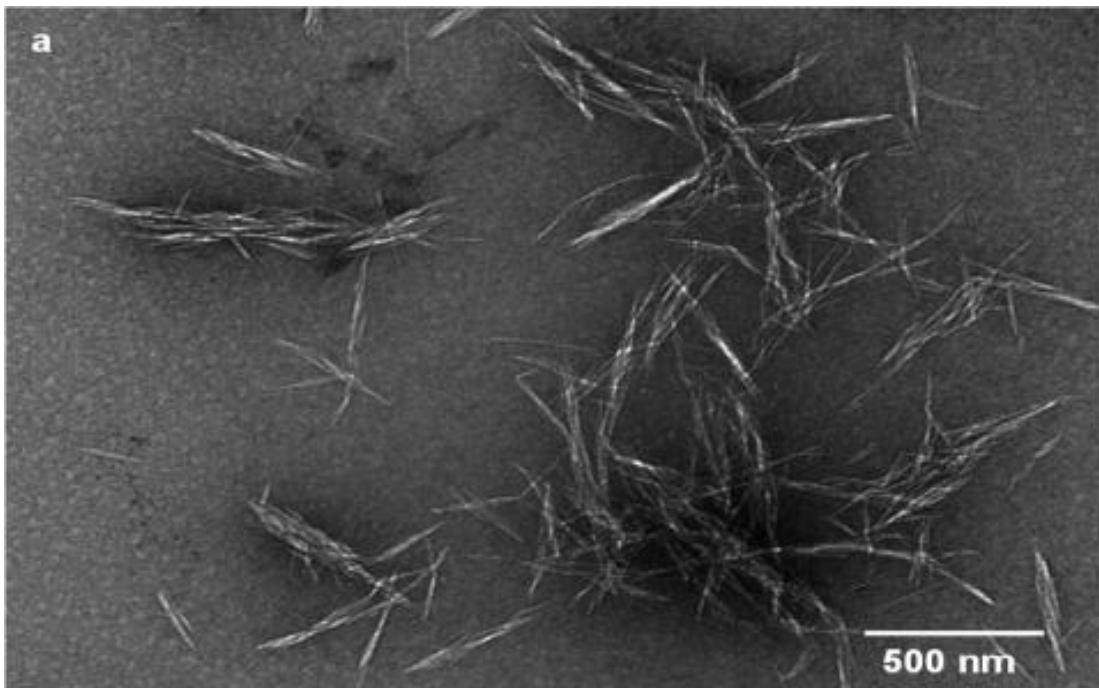


Fig. 4. (a) TEM micrograph CNCs extracted from *Agave* cellulose

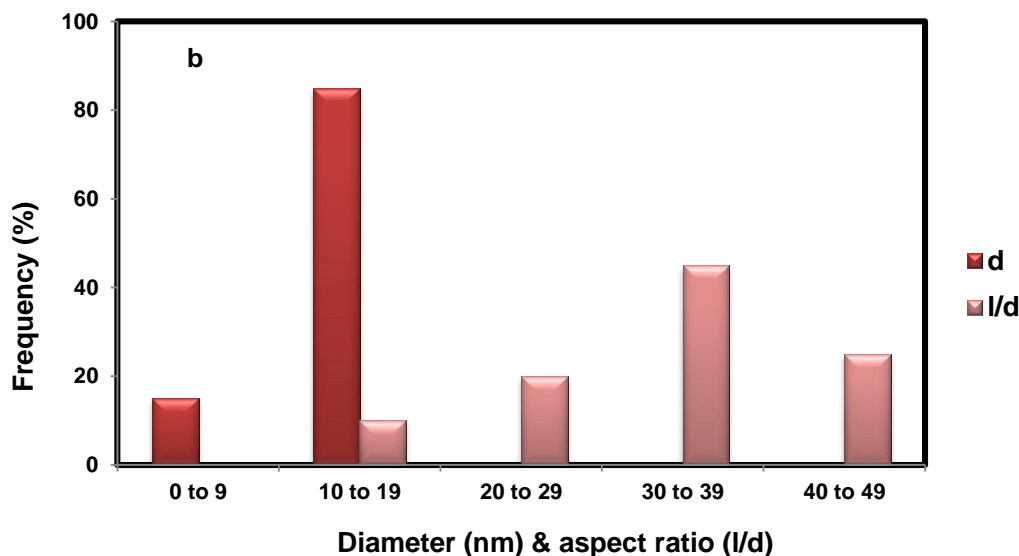


Fig. 4. (b) Diameter and aspect ratio histograms of CNCs extracted from *Agave* cellulose

FTIR Spectroscopy Analysis

The FTIR spectroscopic analysis of the raw and chemically-treated *Agave* fibres is presented in Fig. 5. The changes in infrared absorption indicate that the composition of the fibre had undergone changes during the chemical treatments. The FTIR peak at 1735 cm^{-1} for the raw *Agave* is attributed to the C=O stretching vibration of the acetyl and uronic ester groups, from pectin, hemicelluloses, or the ester linkage of the carboxylic group of ferulic and p-coumaric acids of lignin and/or hemicellulose (Sain and Panthapulakkal 2006; Sun *et al.* 2005). The absorption peak at 1247 cm^{-1} as present in the raw fibre spectra is attributed to the C-O out of plane stretching vibration of the aryl group in the lignin (Troedec *et al.* 2008). These two peaks had completely disappeared in the spectra of the chemically treated fibres. The spectra of cellulose and CNCs showed similar peaks in all wave numbers, the only difference concerning a slight intensity change in the peaks. All of the spectra exhibited a broad band in the region of 3400 to 3300 cm^{-1} , which indicates the free O-H stretching vibration of the OH group in cellulose molecules. In addition, all of the spectra showed the characteristic of C-H stretching vibration around 2900 cm^{-1} (Abdul Khalil *et al.* 2001). Moreover, the vibration peak detected at 1360 to 1375 cm^{-1} in all of the fibre samples is related to the bending vibration of the C-H and C-O bond in the polysaccharide aromatic rings (Nacos *et al.* 2006). Note that the absorbance peaks that are apparent in the spectra in the region of 1627 to 1638 cm^{-1} can be attributed to the O-H bending of the absorbed water (Troedec *et al.* 2008). The peak observed in all of the spectra at 1057 cm^{-1} is due to the C-O-C pyranose ring skeletal vibration. The increase in the intensity of this band showed an increase in crystallinity of the samples (Elanthikkal *et al.* 2010). The most significant absorption band, which continually increases with alkali and bleaching treatment, is 898 cm^{-1} which corresponds to glycosidic -C-H- deformation, with a ring vibration contribution and -O-H bending. These features are characteristic of the β -glycosidic linkage between the anhydroglucose units in cellulose (Alemdar and Sain 2008).

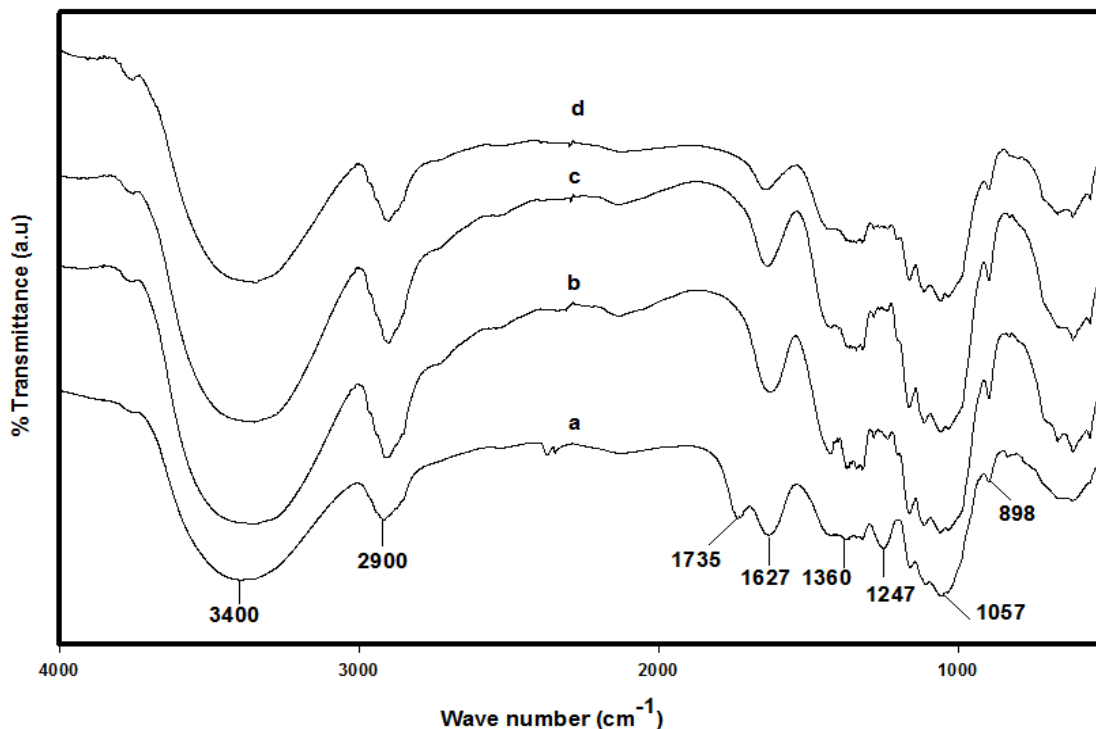


Fig. 5. FTIR spectra of (a) raw, (b) alkali-treated, (c) bleached, and (d) acid-hydrolysed *Agave* fibres

X-ray Diffraction Measurements

Figure 6 shows an X-ray diffraction pattern of the *Agave* fibre and those treated at different stages of the chemical treatments. All of the diffraction patterns showed peaks around $2\theta = 16^\circ$, 22.6° , and 35° , indicating the typical cellulose I structure. The only difference concerns a slight intensity change in the peaks, representing some changes in the fibres crystallinity. For fibres with high cellulose content, like cotton and flax, two peaks around 16° were observed; however, for the raw *Agave* fibres, only one broad peak was observed due to the presence of amorphous material which covered the two peaks (Subramanian *et al.* 2005; Tserki *et al.* 2005). It can be seen in Fig. 6 that the peaks at 16° and 22.6° were more defined for the alkali-treated fibre, and further intensified in the bleached and acid hydrolysed fibre. During the chemical treatment, the cementing materials such as hemicelluloses and lignin were dissolved, and the remaining pure crystalline particles were isolated. These particles gave rise to more intense and narrower crystalline peaks for the chemical treated fibres. Acid hydrolysed cellulose, which shows two peaks at 14° and 16° , like cotton and flax, with a sharp peak at 22.4° , exhibited higher crystallinity due to the more efficient removal of the amorphous parts.

The crystallinity index for the raw, alkali-treated, bleached, and acid-hydrolysed fibres was found to be 59%, 69%, 74%, and 82%, respectively. The results in Table 2 clearly demonstrate the increase in the degree of crystallinity after the chemical treatment. Note that the crystallinity index is used to indicate the order of crystallinity rather than the crystallinity of crystalline regions (Mwaikambo and Ansell 2002). The increase in the crystallinity index is attributed to two effects: (a) the removal of some of the amorphous constituents and (b) the rearrangement of the crystalline regions into a more ordered structure.

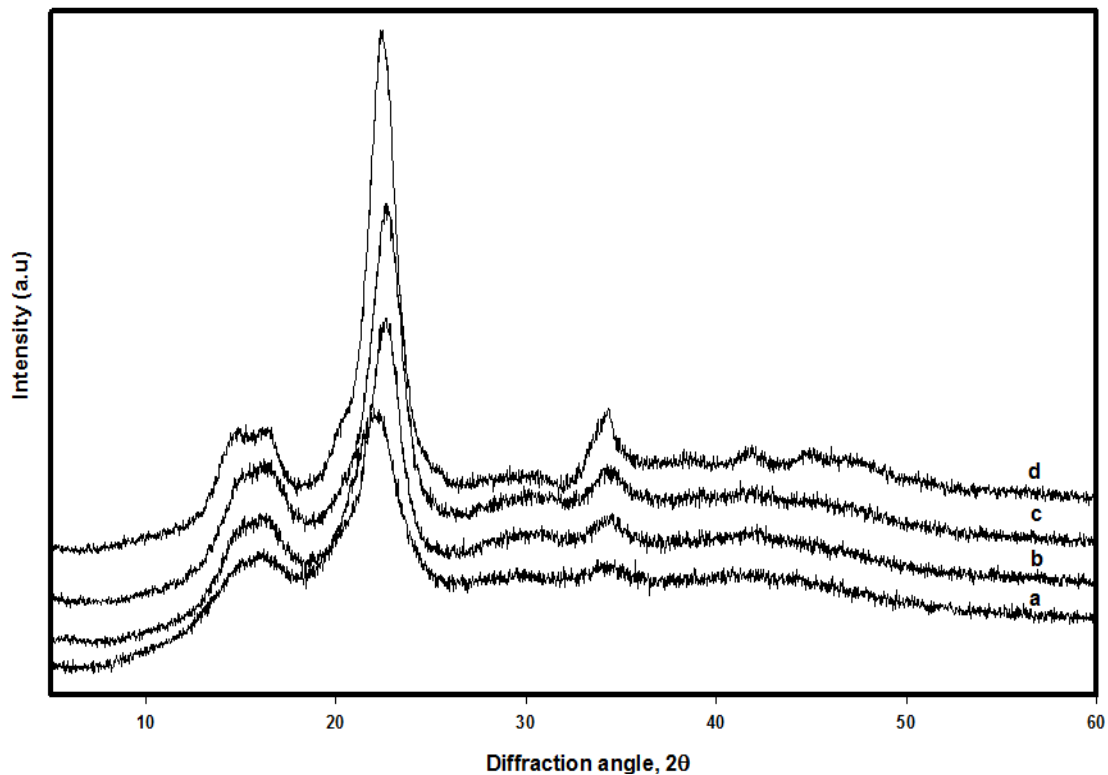


Fig. 6. X-ray diffraction patterns for (a) raw, (b) alkali-treated fibres, (c) bleached, and (d) acid-hydrolysed *Agave* fibres

Table 2. Crystallinity Index of *Agave* Fibres at Different Stages of Chemical Treatment

Fibre stage	2θ (am) (°)	2θ (002) (°)	Crystallinity index (%)
Raw fibres	18.4	22.0	59.0
Alkali-treated fibres	18.4	22.6	69.4
Bleached fibres	18.8	22.6	74.4
Acid hydrolysis	18.2	22.4	82.4

Thermogravimetric Analysis

Thermogravimetric analysis (TGA) was performed to investigate the suitability of the raw and chemically treated *Agave* fibres for biocomposites processing. The thermal behaviour of the lignocellulosic materials depends on their chemical composition, structure, and degree of crystallinity (Fisher *et al.* 2002). The thermal decomposition parameters were determined from the TGA and DTG curves as shown in Figs. 7(a) and 7(b), respectively. The TGA curve of the raw *Agave* fibre showed four degradation steps related to: (i) moisture evaporation, (ii) hemicellulose, (iii) cellulose, and (iv) lignin degradation. The initial weight losses started at 34 °C for all the samples, and were attributed to the evaporation of the moisture in the fibres. The DTG analysis of the raw *Agave* fibre showed that the peaks at 210 °C and 312 °C were caused by hemicelluloses and α -cellulose degradation, respectively (Basak *et al.* 1993). The degradation of the alkali-treated fibre occurred from 250 to 386 °C with a maximum rate at 356 °C, while the bleached fibre degraded in the range of 260 to 398 °C with a maximum rate at 367 °C; both are attributed to cellulose degradation.

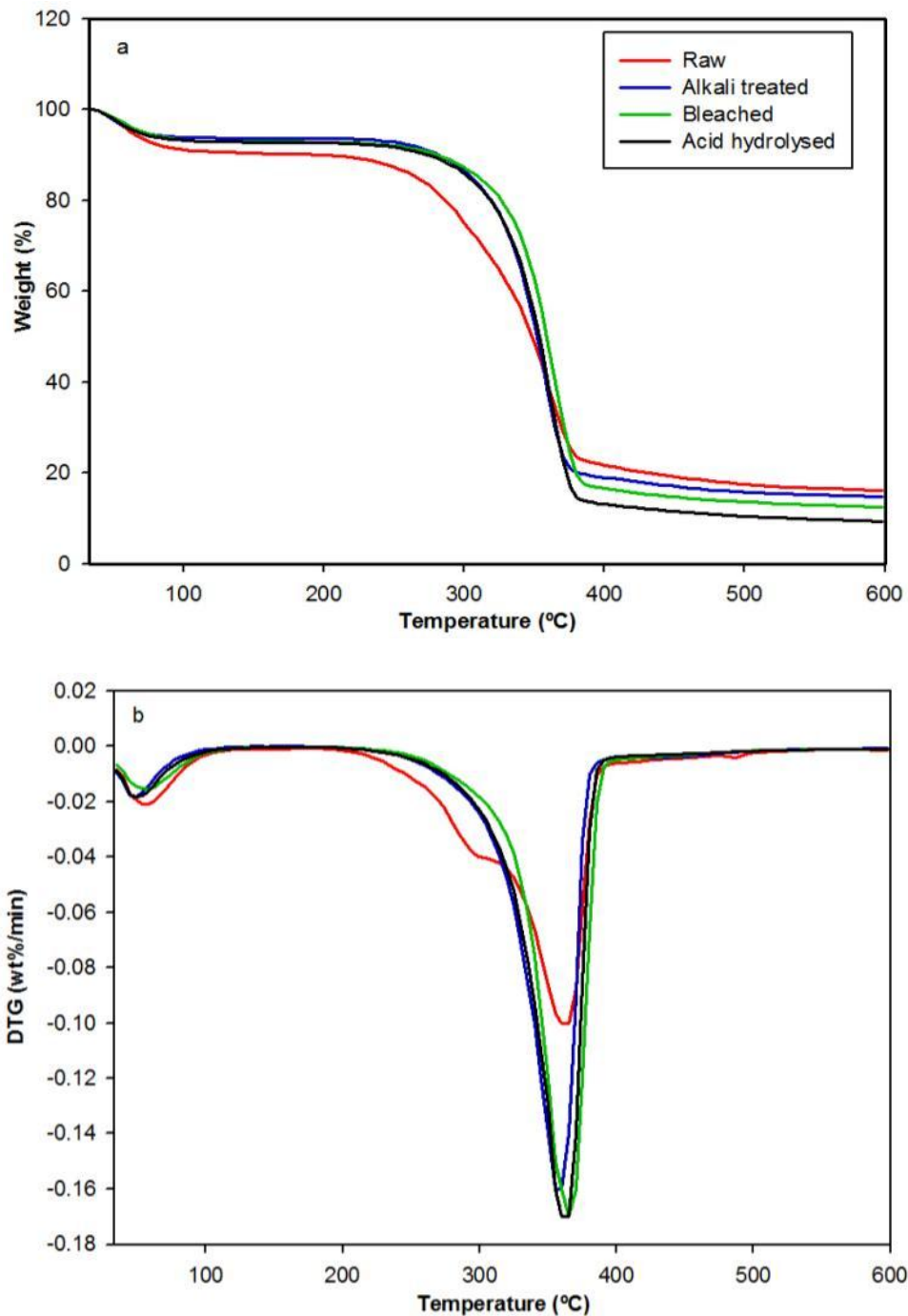


Fig. 7. (a) TGA and (b) DTG curves of raw, alkali-treated, bleached, and acid-hydrolysed *Agave* fibres

The acid-hydrolysed cellulose also showed the same trend as the alkali-treated and bleached fibres with the degradation occurring from 250 to 390 °C with a maximum rate at 361 °C. Based on the thermal stability results of the *Agave* fibres, the results clearly indicated that the degradation temperature increased by chemical treatment, which could be attributed to the removal of hemicelluloses and lignin, as well as a higher degree of crystallinity in the treated fibre samples. The higher crystallinity led to a higher heat

resistance, and improved the thermal degradation. The reduction in the T_{\max} of acid-hydrolysed fibre in comparison to the bleached fibre may correspond to the introduction of sulfate groups into the crystals of cellulose in sulfuric acid hydrolysis (Julien *et al.* 1993). The residue from the degradation step at this onset temperature of degradation was 16, 15, 13, and 12 wt% for raw, alkali-treated, bleached, and acid-hydrolysed cellulose, respectively. The higher amount of residues in the raw *Agave* fibre is due to the presence of lignin as well as ash, which both have a slow degradation rate (Ashori *et al.* 2006). On the other hand, the small amount of residues in the acid hydrolysed cellulose may be the results of the lignin removal during the acid hydrolysis.

CONCLUSIONS

1. Cellulose was extracted from *Agave* fibres by an effective two-step process: the removal of hemicellulose by 4% NaOH and delignification by 1.7% NaClO₂.
2. The isolation of nanocellulose was successfully carried out by acid hydrolysis.
3. The determination of the chemical composition demonstrated the effects of chemical treatments, based on morphological, XRD, FTIR, and TGA analysis.
4. Upon the two-step chemical treatment, the diameter of the fibre was reduced from 230 μm to 7 μm , and thermal stability improved.
5. The cellulose content and crystallinity index increased from 67% and 59% to 97% and 82%, respectively.
6. TEM micrographs suggested that the *Agave* fibres are successfully disintegrated from 7 μm to the range of 8 to 15 nm in diameter, which may have great potential to be used as a reinforcing agent in biocomposite applications.

ACKNOWLEDGEMENT

This work was supported by research grants from the Ministry of Higher Education (MOHE) and Universiti Kebangsaan Malaysia under the research grant GUP-2012-003 and ERGS/1/2012/STG01/UKM/02/4. The authors would also like to thank Dr. Md. Akhir Hamid from Malaysian Agriculture Research & Development Institute (MARDI) for the processing of raw *Agave* fibres.

REFERENCES

- Abdul Khalil, H. P. S., Bhat, A. H., and Yusra, A. F. I. (2011). "Green composites from sustainable cellulose nanofibrils: A review," *Carbohydrate Polymers* 87(2), 963-979.
- Abdul Khalil, H. P. S., Ismail, H., Rozman, H. D., and Ahmad, M. N. (2001). "The effect of acetylation on interfacial shear strength between plant fibre and various matrices," *European Polymer Journal* 37(5), 1037-1045.
- Alemdar, A., and Sain, M. (2008). "Biocomposites from wheat straw nanofibres: morphology, thermal and mechanical properties," *Composites Science and*

- Technology* 68(2), 557-565.
- Ashori, A., Jalaluddin, H., Raverty, W. D., and Mohd Nor, M. Y. (2006). "Chemical and morphological characteristics of Malaysia cultivated kenaf (*Hibiscus cannabinus*) fibre," *Polymer-Plastics Technology and Engineering* 45(1), 131-134.
- Basak, R. K., Saha, S. G., Sarkar, A. K., Saha, M., Das, N. N., and Mukherjee, A. K. (1993). "Thermal properties of jute constituents and flame retardant jute fabrics," *Textiles Research Journal* 63(11), 658-666.
- Bledzki, A. K. and Gassan, J. (1999). "Composites reinforced with cellulose based fibres," *Progress in Polymer Science* 24(2), 221-274.
- Bledzki, K., Reihmane, S., and Gassan, J. (1996). "Properties and modification methods for vegetable fibres for natural fibre composites," *Journal of Applied Polymer Science* 59(8), 1329-1336.
- Elanthikkal, S., Gopalakrishnapanicker, U., Varghese, S., and Guthrie, J. T. (2010). "Cellulose microfibrils produced from banana plant wastes: Isolation and characterization," *Carbohydrate Polymers* 80(3), 852-859.
- Fisher, T., Hajaligol, M., Waymack, B., and Kellogg, D. (2002). "Pyrolysis behaviour and kinetics of biomass derived materials," *Journal of Analytical and Applied Pyrolysis* 62(2), 331-349.
- Frederick, T. W., and Norman, W. (2004). *Natural Fibres, Plastics and Composites*, Kluwer Academic Publishers, New York.
- Jiang, L., and Hinrichsen, G. (1999). "Flax and cotton fibre reinforced biodegradable polyester amide composites. 2. Characterization of biodegradation," *Die Angewandte Makromolekulare Chemie* 268(1), 18-21.
- Johar, N., Ahmad, I., and Dufresne, A. (2012). "Extraction, preparation and characterization of cellulose fibres and nanocrystals from rice husk," *Industrial Crops and Products* 37(1), 93-99.
- Julien, S., Chornet, E., and Overend, R. P. (1993). "Influence of acid pre-treatment (H₂SO₄, HCl, HNO₃) on reaction selectivity in the vacuum pyrolysis of cellulose," *Journal of Analytical and Applied Pyrolysis*, 27(1), 25-43.
- Kalia, S., Kaith, B. S., and Kaur, I. (2009). "Pretreatments of natural fibres and their application as reinforcing material in polymer composites—A review," *Polymer Engineering & Science* 49(7), 1253-1272.
- Kargarzadeh, H., Ahmad, I., Abdullah, I., Dufresne, A., Zainudin, S. Y., and Sheltami, R. M. (2012). "Effects of hydrolysis conditions on the morphology, crystallinity, and thermal stability of cellulose nanocrystals extracted from kenaf bast fibres," *Cellulose* 19(3), 855-866.
- Luo, S., and Netravali, A. N. (1999). "Mechanical and thermal properties of environmental friendly 'green' composites made from pineapple leaf fibres and poly(hydroxybutyrate-co-valerate) resin," *Polymer Composites* 20(3), 367-378.
- Mandal, A., and Chakrabarty, D. (2011). "Isolation of nanocellulose from waste sugarcane bagasse (SCB) and its characterization," *Carbohydrate Polymers* 86(3), 1291-1299.
- Murherjee, P. S. and Satyanarayana, K. G. (1984). "Structure properties of some vegetable fibres, part 1. Sisal fibre," *Journal of Materials Science* 19(12), 3925-3934.
- Mwaikambo, L.Y., and Ansell, M. P. (2002). "Chemical modification of hemp, sisal, jute, and kapok fibres by alkalization," *Journal of Applied Polymer Science* 84(12), 2222-2234.

- Nacos, M., Katapodis, P., Pappas, C., Daferera, D., Tarantilis, P. A., and Christakopoulos, P. (2006). "Kenaf xylan—A source of biologically active acidic oligosaccharides," *Carbohydrate Polymers* 66(1), 126-134.
- Nishino, T., Takano, K., and Nakamae, K., (1995). "Elastic modulus of the crystalline regions of cellulose polymorphs," *Journal of Polymer Science Part B: Polymer Physics* 33(11), 1647-1651.
- Nutman, F. J. (1936). "Agave fibres Pt. I. Morphology, histology, length and fineness; frading problems," *Empire Journal of Experimental Agriculture* 5(75), 75-95.
- Oksmann, K., and Sain, M. (2006). *Cellulose Nanocomposites - Processing, Characterization, and Properties*, Washington, DC: American Chemical Society.
- Rosa, M. F., Medeiros, E. S., Malmonge, J. A., Gregorski, K. S., Wood, D. F., Mattoso, L. H. C., Glenn, G., Orts, W. J., and Imam, S. H. (2010). "Cellulose nanowhiskers from coconut husk fibres: Effect of preparation conditions on their thermal and morphological behaviour," *Carbohydrate Polymers* 81(1), 83-92.
- Rowell, R. M., Young, R. A., and Rowell, J. K. (1997). *Paper and Composites from Agro-based Resources*, CRC Lewis Publishers, Boca Raton FL.
- Sain, M., and Panthapulakkal, S. (2006). "Bioprocess preparation of wheat straw fibres and their characterization," *Industrial Crops and Products* 23(1), 1-8.
- Segal, L., Creely, J. J., Martin, A. E., and Conrad, C. M. (1959). "An empirical method for estimating the degree of crystallinity of native cellulose using the X-ray diffractometer," *Textile Research Journal* 29(10), 786-794.
- Subramanian, K., Kumar, S. P., Jeyapal, P., and Venkatesh, N. (2005). "Characterization of ligno-cellulosic seed fibre from *Wrightia tinctoria* plant for textile applications—An exploratory investigation," *European Polymer Journal* 41(4), 853-861.
- Sun, X. F., Xu, F., Sun, R. C., Fowler, P., and Baird, M. S. (2005). "Characteristics of degraded cellulose obtained from steam-exploded wheat straw," *Carbohydrate Research* 340(1), 97-106.
- Takagi, H., and Asano, A. (2008). "Effects of processing conditions on flexural properties of cellulose nanofibre reinforced "green" composites," *Composites Part A: Applied Science and Manufacturing* 39(4), 685-689.
- Takagi, H., and Ichihara, Y. (2004). "Effect of fibre length on mechanical properties of "green" composites using a starch-based resin and short bamboo fibres," *Japan Society of Mechanical Engineers International Journal, Series A* 47(4), 551-555.
- Troedec, M., Sedan, D., Peyratout, C., Bonnet, J., Smith, A., and Guinebretiere, R. (2008). "Influence of various chemical treatments on the composition and structure of hemp fibres," *Composites Part A - Applied Science and Manufacturing* 39(3), 514-522.
- Tserki, V., Matzinos, P., Kokkou, S., and Panayiotou, C. (2005). "Novel biodegradable composites based on treated lignocellulosic waste flour as filler. Part I. Surface chemical modification and characterization of waste flour," *Composites Part A: Applied Science and Manufacturing* 36(9), 965-974.
- Wise, L. E., Murphy, M., and D'Addieco, A. A. (1946). "Chlorite, holocellulose, its fractionation and bearing on summative wood analysis and on studies on the hemicelluloses," *Paper Journal* 122(2), 35-43.

Article submitted: Dec. 16, 2012; Peer review completed: Jan. 25, 2013; Revised version received and accepted: Feb. 18, 2013; Published: Feb. 21, 2013.